EXCITONIC LIGHT EMISSION DECAY TIME MEASUREMENTS IN MODERATELY δ-DOPED GaAs/AlAs MULTIPLE QUANTUM WELLS

J. Kundrotas [a], A. Čerškus [a], G. Valušis [a], E.H. Linfield [b], E. Johannessen [c],

and A. Johannessen [c]

[a] *Semiconductor Physics Institute of Center for Physical Sciences and Technology, A. Goštauto 11, LT-01108 Vilnius, Lithuania*
[b] *School of Electronic and Electrical Engineering, University of Leeds, Leeds LS2 9JT, United Kingdom*
[c] *Buskerud and Vestfold University College, Raveien 215, 3184 Borre, Norway*
E-mail: aurimas.cerskus@ftmc.lt

The radiative recombination rate of moderately doped *n*-type and *p*-type GaAs/AlAs multiple quantum wells using a time-correlated single photon counting system is presented. The experimental study has been obtained within a wide temperature range from liquid helium to room temperature and the work has focused on identifying photoluminescence decay rates based on free-exciton recombinations. It was found that the free exciton decay time was reduced in doped multiple GaAs/AlAs quantum wells, and that the reduction rate depends on both the concentration and doping type.

Keywords: quantum well, photoluminescence, lifetime

PACS: 78.55.-m, 78.67.De, 78.47.jd

1. Introduction

The optical properties of GaAs/AlAs quantum wells (QWs) are governed by excitons over the temperature range spanning liquid helium to room temperature. In quantum wells the two-dimensional exciton has both a large binding energy and a strong oscillator strength in comparison with a bulk semiconductor. This is related to the quantum confinement of wave functions between created potential barriers.

The optical properties of quantum wells can be divided into two groups. The first group covers the intrinsic properties related to excitonic transitions and free carrier transitions from the conduction band to the valence band. The other group deals with extrinsic optical properties related to impurity induced optical transitions such as a free electron to a neutral acceptor or a free hole to a neutral donor. However, the impurities would also influence the intrinsic optical properties, form impurity bound excitons, change the excitonic emission line width and the light emission decay time. It is therefore of fundamental importance to understand the effect of impurities in order to determine the electronic, optical and transport properties of doped QWs. The radiative emission processes of carriers in QWs are of the most importance in order to determine various recombination mechanisms.

The experimental and theoretical dynamics of excitonic emission have been extensively reported in literature [1]. Researchers have also focused on the dynamics of formation of excitons in QWs both experimentally [2–5] and theoretically [6–8]. It was concluded that the excitons form with a time constant extending from about 10 picoseconds and up to a few hundred picoseconds depending on the experimental conditions used. The same applies also for the free exciton lifetimes in QWs. The investigation of the excitonic lifetime phenomena has been reported both experimentally [9–15] and

theoretically [16–18], and it has been shown that this depends on the excitation condition (resonantly or nonresonantly), the quantum well width and the lattice temperature. The lifetimes of nonresonantly excited excitons are found in the region of 0.1–1 ns at liquid helium temperatures depending on the width of the quantum wells and increase linearly with temperatures up to 20–50 K. In contrast, typical radiation lifetime of free excitons in GaAs QWs is short and is of the order of 10 ps. However, this value is not obtained by simple experimental methods on time-resolved photoluminescence (PL), and instead the radiative lifetime of free excitons has been directly measured in very high quality GaAs QWs under resonant excitation conditions [14]. In general, exciton scattering due to alloy disorder, interface roughness or other imperfections leads to a decrease in the exciton coherence length, which results in an enhancement of the radiative lifetime towards the nanosecond time regime.

Impurities in quantum wells may introduce new recombination centers such as bound excitons, initiate new free electron–acceptor or free hole–donor light emission transitions as well as reduce the band-to-band and excitonic emission dynamics [19–26]. The magnitude and level of these effects will depend on the type and concentration of the impurities used. We note that in moderately doped QWs the shortest lifetime at low temperatures is the excitonic emission lifetime in comparison with lifetimes of free carriers – neutral impurity related optical transitions [19–21].

The properties of weakly or moderately doped QWs can initially be explained by a model assuming that impurities are noninteracting, but as the impurity concentration increases, one reaches a situation where the single-impurity theory is no longer valid. This effect is caused by the overlap of the impurity wave functions, where the formation of the impurity band causes tails to form at the edge of the first conduction or valence sub-band edge depending on the dopant being *n*-type or *p*-type. At a very high doping concentration, the impurity band will overlap with the free-carrier continuum, and this threshold corresponds to the Mott transition from insulating to the metallic behaviour of the carriers [27]. The recombination processes near or over the Mott transition of *p*-type GaAs multiple quantum wells are described in Refs. [28, 29].

This paper presents the results from studies on moderately doped GaAs/AlAs multiple quantum wells with impurity concentrations below the Mott transition level. The work has focused on the investigation of the time-resolved intrinsic PL properties of silicon (Si) and beryllium (Be) δ-doped GaAs/AlAs MQWs over a wide temperature range from liquid helium to room temperature.

2. Samples and experimental setup

The silicon or beryllium δ-doped multiple quantum wells were grown by molecular beam epitaxy on semi-insulating GaAs substrates. The samples contained a fixed number of wells ($N = 40$), with widths (L_W) of 20 nm and separated by 5 nm thick AlAs barriers. Each of the QWs was δ-doped (about 2 nm width) with Si donors or Be acceptors at the center of the well. The doping level for the Si doped MQWs was 4.0×10^9, 1.0×10^{10} and 1.4×10^{11} cm^{-2}, respectively; whereas for the Be doped MQWs it was 5.0×10^{10} and 2.5×10^{12} cm^{-2}, respectively.

The continuous wave (CW) PL spectra were measured by a monochromator. The spectral resolution of the wavelength was 0.008 nm at a monochromator exit slit width of 10 μm, and the corresponding spectral resolution of the energy was 0.015 meV at 820 nm (1.512 eV). An Ar-ion laser was used as the excitation source with excitation energy in the range of 2.2–2.7 eV or a CW diode-pumped solid-state (DPSS) laser of 2.71 eV (457 nm). The PL was detected by a *Hamamatsu* GaAs photomultiplier or a high efficiency extended red multialkali cathode photomultiplier, both operating in the photon counting regime and being thermoelectrically cooled.

The time-resolved PL measurements were performed using a frequency-doubled diode-pumped Nd:LSB solid-state microchip laser with an FWHM pulse width of 400 ps. The pulse repetition rate was 10 kHz, while the average output power was set to 40 mW. The excitation wavelength was 531 nm (photon energy of 2.3 eV). The transient PL was measured with a time-correlated single photon counting (TCSPC) system, whereas the excitation intensity was varied by using neutral glass filters in the path of the laser beam.

The initial electrical time resolution of the TCSPC module was with an FWHM of 8 ps. However, due to the finite width of the laser pulse and finite resolution of the photomultiplier, the FWHM of the instrument response function (IRF) increased up to 400 ps. Nevertheless, the lifetimes 10 times shorter than the IRF width can be measured using deconvolution.

The characteristic decay times were extracted by incorporating one or two exponential decay time constants to the PL decay transient curves. For short lifetimes, a standard numerical deconvolution procedure was used.

The free exciton radiative lifetime can be measured from the fundamental relationship between the radiative lifetime and the spectral linewidth [9]. However, this can only be estimated under the main assumption that the nonradiative processes play a negligible role in recombination [10]. It is also important to note that the relationship between the radiative lifetime and spectral linewidth can only be considered for free excitons and for very high quality quantum wells.

The sample temperatures were changed from ambient room temperature (300 K) down to 3.6 K using a closed cycle helium optical cryostat. The cryostat was equipped with two thermometers; the first one was used to control the operation of the equipment and the second one was used to measure the temperature of the sample. More details of the experimental setup can be found in [21].

3. Experimental results and discussion

The CW PL spectra of the Si donor and Be acceptor doped MQWs samples performed at 3.6 K, 77 K and 300 K are presented in Figs. 1–3. A series of clearly resolved peaks can be seen. The most intensive PL bands are associated with heavy- and light-hole excitonic transitions denoted as $X_{e1\text{-}hh1}$ and $X_{e1\text{-}lh1}$, respectively.

The lower energy transitions of Si doped MQWs, labelled as Si-h, are attributed to the recombination of free holes and electrons bound to a Si donor. The line labelled as [SiX] is ascribed to excitons bound to a Si donor impurity. These lines disappear at higher liquid nitrogen and room temperatures. The excitonic lines dominate in the silicon doped MQWs, and their strength is weakly related to the doping concentration.

The lower energy transitions of Be acceptor doped MQWs, labelled as e-Be, are attributed to the recombination of free electrons and holes bound to a Be acceptor. It is also possible to discriminate the line originating from the exciton bound to the acceptor impurity, labelled as [BeX]. It can be observed that this line dominates at low temperatures. At liquid nitrogen and room temperatures some additional lines appear in the spectrum. However, they are shifted to the lower energy side due to the temperature dependency of the forbidden energy gap of the QWs. At low temperatures, the free excitonic line strength of the Be acceptor doped QWs expresses strong dependence on the acceptor doping concentration in contrast to the Si donor doped QWs.

In GaAs/AlAs MQWs, both heavy-hole and light-hole excitonic peaks are almost merged together at
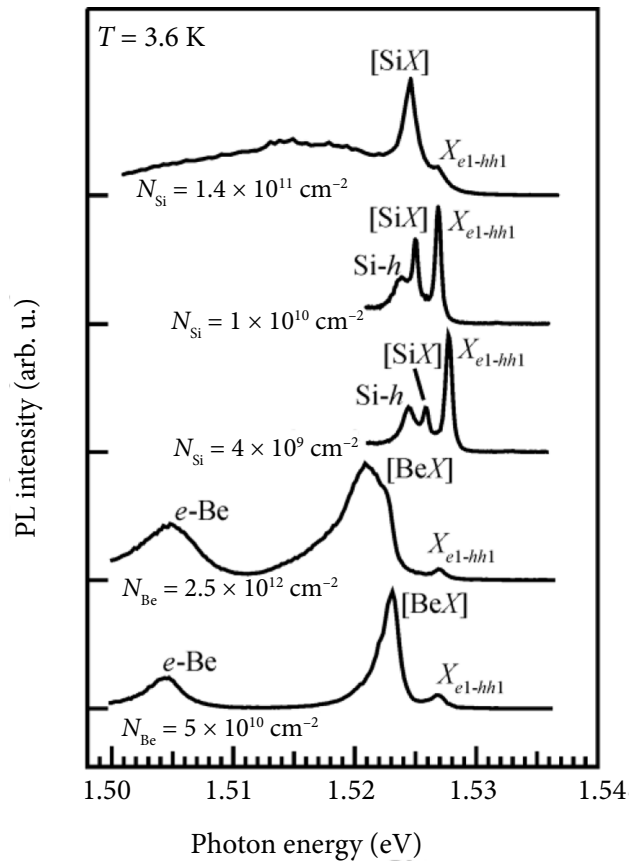

Fig. 1. The CW PL spectra at 3.6 K for the Si and Be δ-doped GaAs/AlAs MQWs (L_W = 20 nm) with a doping concentration of N_{Si} = 4 × 10^9, 1 × 10^{10}, 1.4 × 10^{11} cm^{-2} and N_{Be} = 5 × 10^{10}, 2.5 × 10^{12} cm^{-2}. The symbols $X_{e1\text{-}hh1}$ and $X_{e1\text{-}lh1}$ indicate heavy-hole and light-hole excitonic transitions, respectively, [SiX] is the Si donor-bound exciton, Si-h is the free hole-neutral Si donor transitions, [BeX] is the Be acceptor-bound exciton, and e-Be is the free electron-neutral Be acceptor transitions. The curves are offset vertically for clarity.

room temperature. However, it allows one to discriminate the line $E_{e2\text{-}hh2}$, related to transitions between the second sublevels. The arrows (Fig. 3) indicate the calculated values of these energy sublevels. More details about the experimental investigation and theoretical analysis of Si and Be doped MQWs CW PL spectra can be found in 30–32].

The PL decay transients of the $X_{e1\text{-}hh1}$ heavy-hole excitonic emission bands for the Si and Be δ-doped samples with different doping concentrations are shown in Figs. 4–8 at a temperature of T = 3.6, 20, 77 and 300 K. A laser pulse excitation intensity of I_{imp} = 70 W/cm^2 was used. The average pulse excitation intensity was about 0.28 mW/cm^2. The electron–hole pairs are generated nonresonantly both in the QWs and in the barriers.
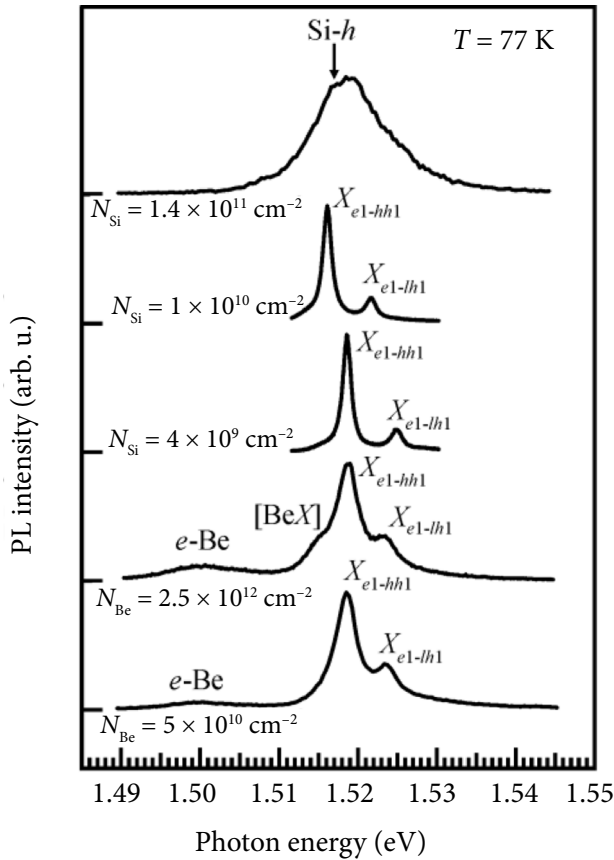
Fig. 2. The CW PL spectra at liquid nitrogen temperature of the Si and Be δ-doped GaAs/AlAs MQWs (L_{W} = 20 nm) with a doping concentration of $N_{\mathrm{Si}} = 4 \times 10^9$, 1×10^{10}, 1.4×10^{11} cm^{-2}, and $N_{\mathrm{Be}} = 5 \times 10^{10}$, 2.5×10^{12} cm^{-2}. The same symbols are used as in Fig. 1. The curves are offset vertically for clarity.

Fig. 3. The CW PL spectra at room temperature for the Si and Be δ-doped GaAs/AlAs MQWs (L_{W} = 20 nm) with a doping concentration of $N_{\mathrm{Si}} = 4 \times 10^9$, 1×10^{10}, 1.4×10^{11} cm^{-2} and $N_{\mathrm{Be}} = 5 \times 10^{10}$, 2.5×10^{12} cm^{-2}. Arrows indicate $E_{e1\text{-}hh1}$, $E_{e2\text{-}hh2}$, and $E_{e1\text{-}lh1}$, that are the calculated energy differences from the first heavy-hole to the first electron, the second heavy-hole to the second electron and the first light-hole to the first electron energy levels, respectively. The curves are offset vertically for clarity.

It can be seen that the measured PL decay time is considerably longer than the rise time and hence is not influenced by the rise time of the luminescence transient. Therefore the measured time evolution in the first 100 ps contains all necessary information about the incoherent nonequilibrium exciton dynamics [15]. Two exponential decay times are observed at low temperatures. The short PL decay time may be related to the filling of the capture centers by free carriers. This phenomenon depends on the excitation intensity (although the dependency of the decay time on excitation intensity was not observed in the experiments performed). Instead, the short lifetimes detected may be attributed to the recombination of non-thermalized excitons at k equal to zero. In contrast, the long PL decay time is related to the lifetime of thermalized excitons. Considering the previous work reported on the excitonic recombination characteristic time [21], this may be attributed to the emission time of the non-thermalized ex-
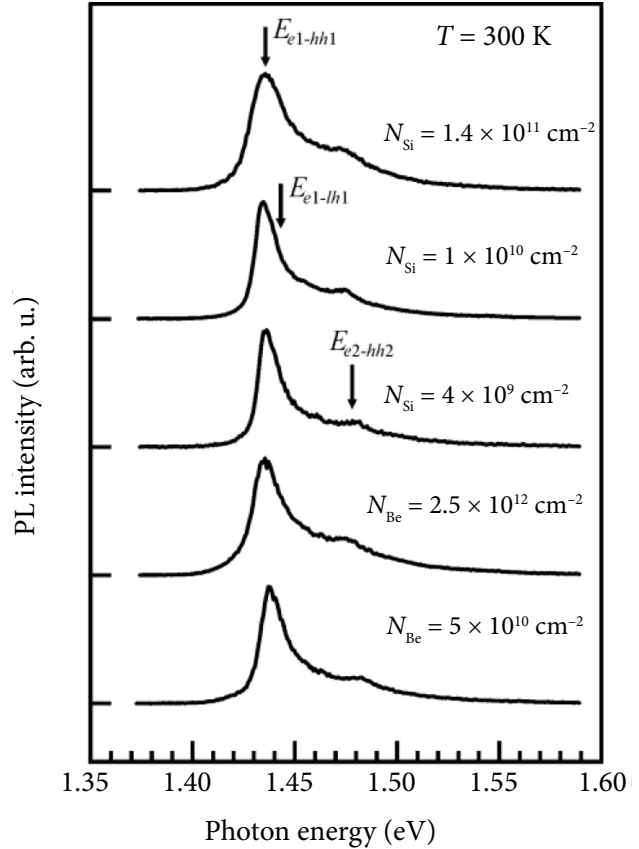
citons. Similar experimental results and a thorough discussion on the recombination of free excitons at low temperature are presented in Ref. [23]. The population of excitons takes a certain time to thermalize to the lattice temperature, and, as thermalization occurs, there is a decrease in the population that is able to recombine due to momentum conservation restrictions. This is due to the thermalization of excitons requiring the interaction of excitons with phonons. Our results suggest that this complicated recombination process of free excitons is less apparent at higher temperatures since the thermalization time becomes shorter and the decay characteristic time can be considered as one-exponential process. Measuring the carrier temperatures directly from the heavy-hole exciton line is not possible since luminescence occurs only near k equal to zero [33].
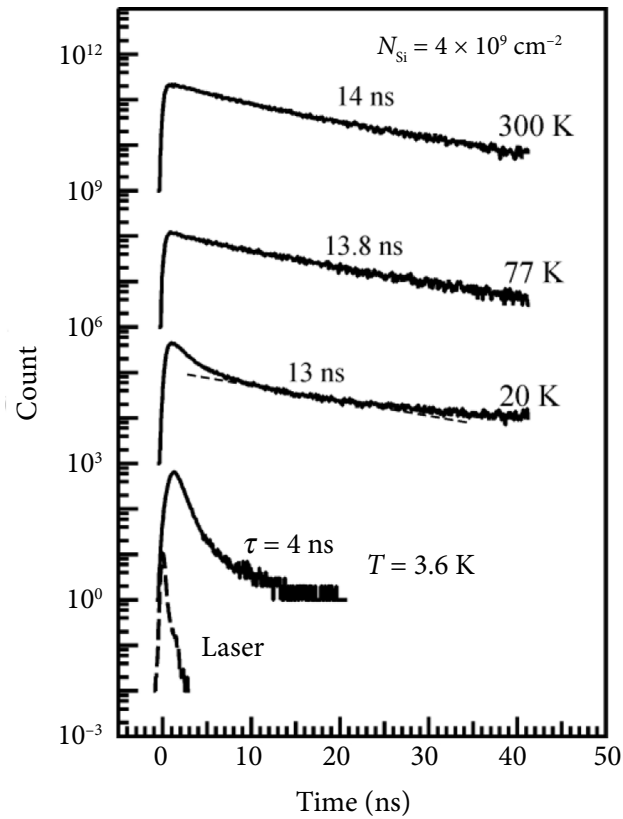
Fig. 4. The PL decay transients of $X_{e1\text{-}hh1}$ heavy-hole excitonic emission bands for the lowest Si δ-doped ($N_{Si} = 4.0 \times 10^9$ cm^{-2}) MQWs recorded at $T = 3.6, 20, 77,$ and 300 K with a laser excitation intensity of $I_{imp} = 70$ W/cm^2. The lowest curve indicates the response of the laser excitation pulse. The decay time constants are marked for each trace. The curves are offset vertically for clarity.

Fig. 5. The PL decay transients of $X_{e1\text{-}hh1}$ heavy-hole excitonic emission bands for the second Si δ-doped ($N_{Si} = 1.0 \times 10^{10}$ cm^{-2}) MQWs recorded at $T = 3.6, 20, 77,$ and 300 K with a laser excitation intensity of $I_{imp} = 70$ W/cm^2. The lowest curve indicates the response of the laser excitation pulse. The decay time constants are marked for each trace. The curves are offset vertically for clarity.

In further investigations we will examine this long PL decay time and will prove that this long PL decay time depends not only on the temperature but also on the doping concentration and doping type (*n*-type or *p*-type).

The photoluminescence decay time at the heavy-hole excitonic $X_{e1\text{-}hh1}$ emission position in the *n*-type GaAs/AlAs ($L_W = 20$ nm) MQWs is presented in Fig. 9. Three different doping concentrations of Si have been considered ($N_{Si} = 4 \times 10^9, 1 \times 10^{10}, 1.4 \times 10^{11}$ cm^{-2}) as a function of temperature in the range from 3.6 to 300 K. The maximum value of the emission decay time constant of weakly doped quantum wells with a doping concentration of $N_{Si} = 4 \times 10^9$ cm^{-2} was measured to be approx. 16 ns at a temperature of 40 K. The tendency of a decrease in the free exciton decay time in higher doped samples is also visible in Fig. 9. At higher temperatures, the observed decay time is not clearly based on the excitonic lifetime, but consists instead of two
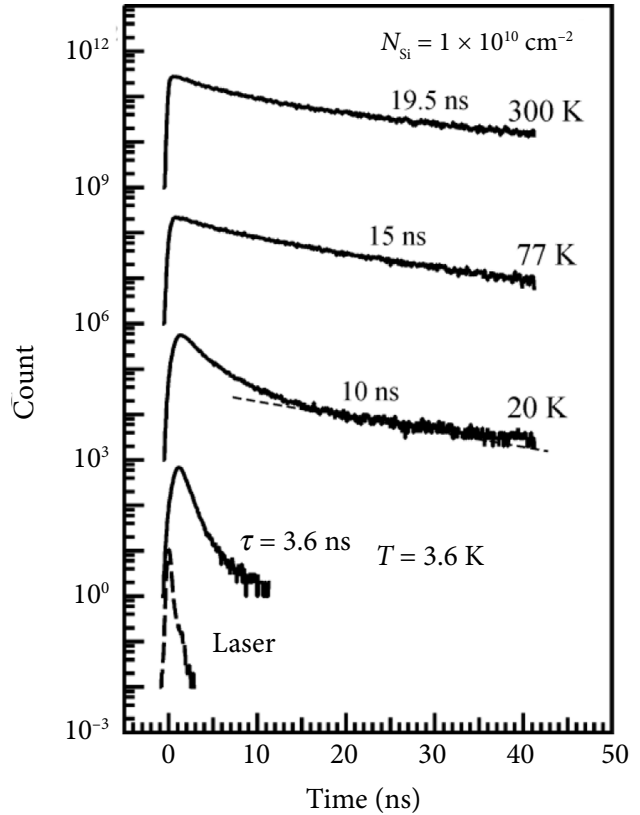
components (radiative and nonradiative). The nonradiative lifetime is initially related to the recombination of free carriers without the emission of photons. At higher temperatures the concentration of free carriers is increased due to the influence of optical phonons that ionizes the excitons and dissolves them into free carriers. This will increase the nonradiative recombination of thermally generated free carriers which leads to a saturation of the measured excitonic line emission decay time and consequently a reduction of temperature dependent variations at elevated higher temperatures.

The nonradiative lifetime is also a signature of imperfections of quantum wells at higher temperatures (the concentration of imperfections depends on technology conditions, for example, growth temperature). This influence can be observed especially in *n*-type doped samples. In spite of the fact that the second *n*-type samples ($N_{Si} = 1 \times 10^{10}$ cm^{-2}) are more intensively doped, the PL decay time at room

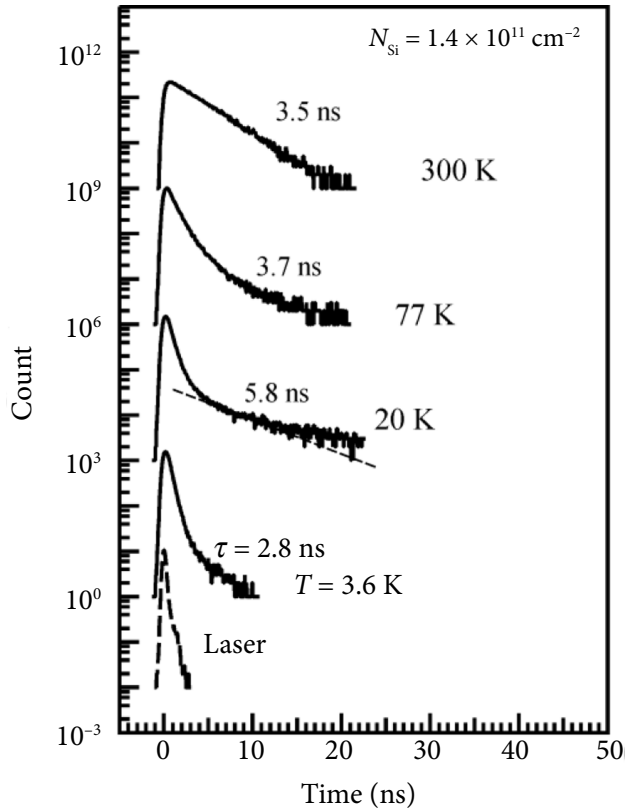Fig. 6. The PL decay transients of $X_{e1\text{-}hh1}$ heavy-hole excitonic emission bands for the third Si δ-doped ($N_{Si} = 1.4 \times 10^{11}$ cm^{-2}) MQWs recorded at $T = 3.6, 20, 77$, and 300 K with a laser excitation intensity of $I_{imp} = 70$ W/cm^2. The lowest curve indicates the response of the laser excitation pulse. The decay time constants are marked for each trace. The curves are offset vertically for clarity.

Fig. 7. The PL decay transients of $X_{e1\text{-}hh1}$ heavy-hole excitonic emission bands for the lowest Be δ-doped ($N_{Be} = 5.0 \times 10^{10}$ cm^{-2}) MQWs recorded at $T = 3.6, 20, 77$, and 300 K with a laser excitation intensity of $I_{imp} = 70$ W/cm^2. The lowest curve indicates the response of the laser excitation pulse. The decay time constants are marked for each trace. The curves are offset vertically for clarity.

temperature is longer in comparison with the first sample ($N_{Si} = 4 \times 10^9$ cm^{-2}). The first sample was grown at substrate temperature $T_s = 570$ °C, whereas the second sample at $T_s = 595$ °C. Due to different growth conditions, it is expected that the longer PL decay time of the second sample is a result of a lower concentration of nonradiative recombination centers.

The photoluminescence decay time at the heavy-hole excitonic emission $X_{e1\text{-}hh1}$ position in the p-type GaAs/AlAs ($L_W = 20$ nm) MQWs for two different Be concentrations ($N_{Be} = 5 \times 10^{10}$ and 2.5×10^{12} cm^{-2}) is presented in Fig. 10. This decay time for both doping concentrations was measured as a function of temperature in the range of 3.6 to 300 K. The maximum decay time constant was measured to be about 12 ns at 150 K for weakly doped quantum wells with a doping concentration of $N_{Be} = 5 \times 10^{10}$ cm^{-2}. It can also be seen from Fig. 10 that the free exciton decay time in the higher doped sample is shorter. At higher temperatures, the observed decay time is independ-
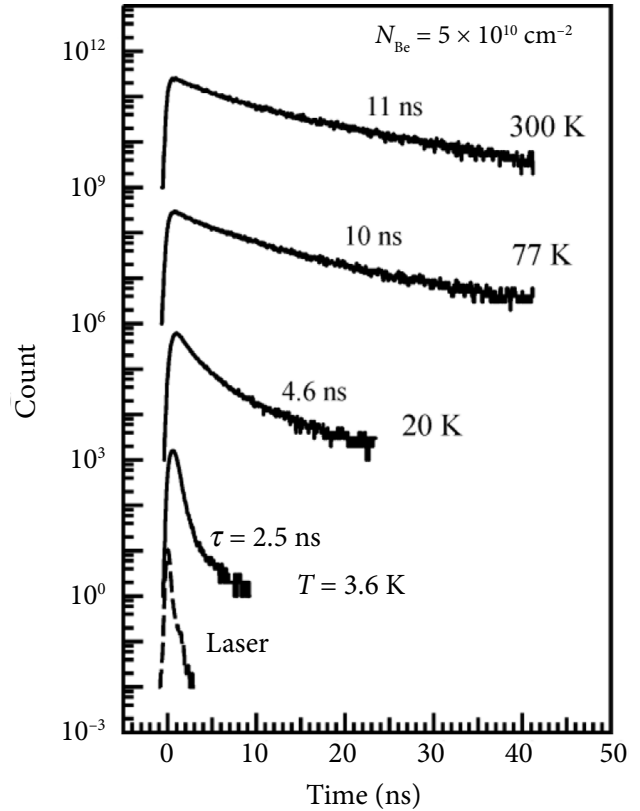
ent of temperature and it is not clearly excitonic lifetime as in n-type QWs. For the higher doped sample nonradiative recombination of free carriers begins to dominate at lower temperature and the saturation of decay time is achieved at lower temperature.

The results presented in both Figs. 9 and 10 allows one to draw an important conclusion: for the highest doped n-type $N_{Si} = 1.4 \times 10^{11}$ cm^{-2} and p-type doped $N_{Be} = 2.5 \times 10^{12}$ cm^{-2} samples the saturation of emission decay time begins at similar temperature $T = 30$ K, but at different doping levels. It is worth noting that for the n-type sample the Si concentration is lower by about one order than the concentration for Be p-doped samples. The saturation of emission decay time indicates that impurities create nonradiative recombination centers. A question arises: why does the nonradiative recombination begin to dominate at different concentration for n-type and p-type MQWs? It can be supposed that this effect is related to an overlap of impurity wave functions as well as collective effects.
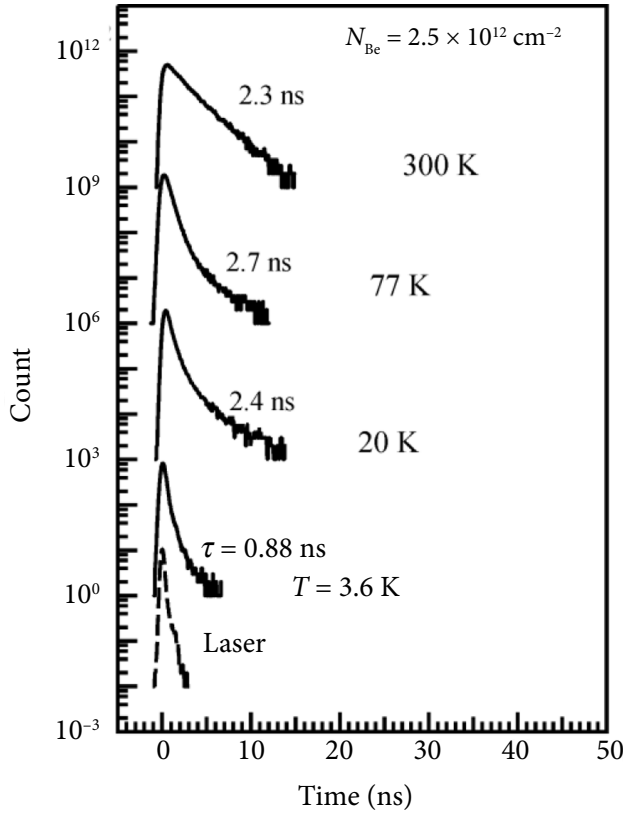
Fig. 8. The PL decay transients of $X_{e1\text{-}hh1}$ heavy-hole excitonic emission bands for the second Be δ-doped ($N_{Be} = 2.5 \times 10^{12}\,\mathrm{cm^{-2}}$) MQWs recorded at $T = 3.6$, 20, 77, and 300 K with a laser excitation intensity of $I_{imp} = 70\,\mathrm{W/cm^2}$. The lowest curve indicates the response of the laser excitation pulse. The decay time constants are marked for each trace. The curves are offset vertically for clarity.
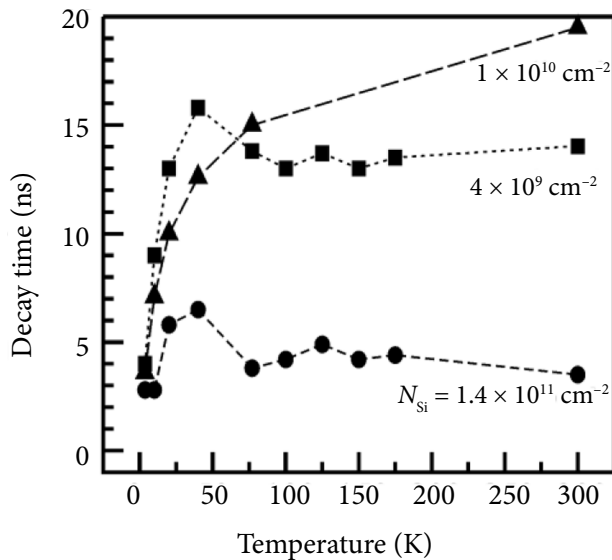
As mentioned in the introduction, the properties of weakly or moderately doped QWs can be explained by a model assuming that the impurities are noninteracting. However, as the impurity concentration increases, the overlap of the impurity wave functions becomes more and more significant and leads to a metal–insulator Mott transition [27].

In previous experiments [32], considering GaAs/AlAs MQWs ($L_W = 20$ nm), the Si donor binding energy was found to be $E_D \approx 11.6$ meV and the Be acceptor binding energy was found to be $E_A \approx 30$ meV. From the binding energies, the calculated Bohr radius of the Si donor is equal to $a_{Si} \approx 5$ nm and for the Be acceptor it is equal to $a_{Be} \approx 1.9$ nm. These results enable calculation of the critical concentration of the Mott transition [28, 29]. Our estimations show that the Mott transition in the Si *n*-type GaAs/AlAs QWs ($L_W = 20$ nm) occurs at a concentration of $N_{Si} = 4 \times 10^{11}\,\mathrm{cm^{-2}}$, whereas in the Be *p*-type GaAs/AlAs QWs ($L_W = 20$ nm) it occurs at a concentration of $N_{Be} = 2.7 \times 10^{12}\,\mathrm{cm^{-2}}$. These concentrations differ by approx. one order of magnitude for the *n*-type and *p*-type impurities. This is related to different ionization energies and different Bohr radius of the donor and the acceptor. Since the donor-like impurities are more shallow (have a larger Bohr radius), the Mott transition occurs at a lower concentration in comparison to the acceptor-like impurities. The highest doped *n*-type ($N_{Si} = 1.4 \times 10^{11}\,\mathrm{cm^{-2}}$) and *p*-type ($N_{Be} = 2.5 \times 10^{12}\,\mathrm{cm^{-2}}$) samples have the impurity concentration near the Mott transition threshold.

Fig. 9. Photoluminescence decay time at the heavy-hole excitonic emission $X_{e1\text{-}hh1}$ position in the *n*-type MQWs ($N_{Si} = 4 \times 10^9$, 1×10^{10}, $1.4 \times 10^{11}\,\mathrm{cm^{-2}}$) as a function of temperature. The dashed lines are a guide for the eye.
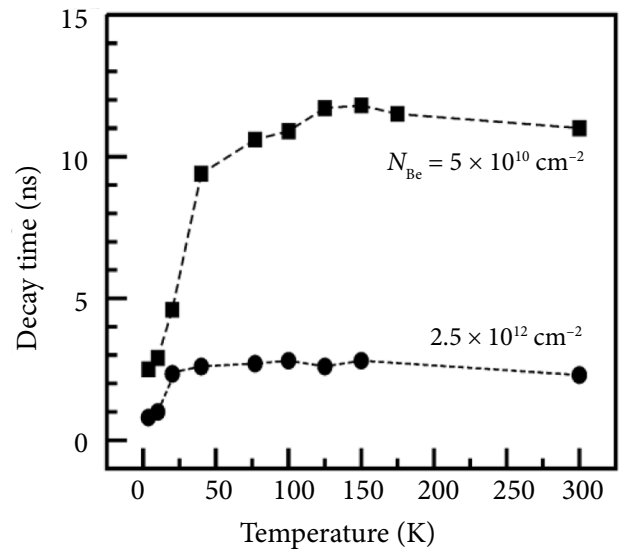

Fig. 10. Photoluminescence decay time at the heavy-hole excitonic emission $X_{e1\text{-}hh1}$ position in *p*-type MQWs ($N_{Be} = 5 \times 10^{10}$, $2.5 \times 10^{12}\,\mathrm{cm^{-2}}$) as a function of temperature. The dashed lines are a guide for the eye.

However, free and bound excitons still form in those MQWs, but also the nonradiative recombination rate increases.

4. Conclusions

The photoluminescence decay time of $X_{e1\text{-}hh1}$ heavy-hole excitonic emission bands from Si and Be δ-doped GaAs/AlAs MQWs ($L_W = 20$ nm) for ($N_{Si} = 4 \times 10^9$, 1×10^{10}, 1.4×10^{11} cm^{-2}) and ($N_{Be} = 5 \times 10^{10}$, 2.5×10^{12} cm^{-2}) was measured as a function of temperature within the range from 3.6 up to 300 K. It was found that the free exciton radiation lifetime is related to the lifetime of thermalized heavy-hole excitons in the temperature region of up to 50 K. In this temperature range, the radiation lifetime increases linearly with temperature. Above 50 K, the nonradiative recombination of free carriers dominates and the PL decay time approaches saturation (dependent on the impurity concentration). The existence of impurity threshold concentration leads to an intensive growth of nonradiative recombination, and this induces a shorter PL decay time at higher temperatures compared to that of lightly doped QWs. This is related to an overlap of the impurity wave functions near the Mott transition, which for the Si n-type doped GaAs/AlAs QWs ($L_W = 20$ nm) occurs at a concentration of $N_{Si} = 4 \times 10^{11}$ cm^{-2} and for the Be p-type doped GaAs/AlAs QWs ($L_W = 20$ nm) it occurs at a concentration of $N_{Be} = 2.7 \times 10^{12}$ cm^{-2}. For such highly doped samples, the collective effects of impurities will start to play a more important role in the recombination processes.

References

[1] J. Shah, *Ultrafast Spectroscopy of Semiconductors and Semiconductor Nanostructures*, 2nd ed. (Springer-Verlag, Heidelberg, 1999).

[2] T.C. Damen, J. Shah, D.Y. Oberli, D.S. Chemla, J.E. Cunningham, and J.M. Kuo, Dynamics of exciton formation and relaxation in GaAs quantum wells, Phys. Rev. B. **42**, 7434–7438 (1990).

[3] R. Kumar, A.S. Vengurlekar, S.S. Prabhu, J. Shah, and L.N. Pfeiffer, Picosecond time evolution of free electron-hole pairs into excitons in GaAs quantum wells, Phys. Rev. B **54**, 4891–4897 (1996).

[4] J. Szczytko, L. Kappei, J. Berney, F. Morier-Genoud, M.T. Portella-Oberli, and B. Deveaud, Determination of the exciton formation in quantum wells from time-resolved interband luminescence, Phys. Rev. Lett. **93**, 137401 (2004).

[5] E. Kozhemyakina, K. Zhuravlev, A. Amo, and L. Viña, Exciton-formation time obtained from the spin splitting dynamics, J. Phys. Conf. Ser. **210**, 012002 (2010).

[6] A. Thilagam and J. Singh, Generation rate of 2D excitons in quantum wells, J. Lumin. **55**, 11–16 (1993).

[7] C. Piermarocchi, F. Tassone, V. Savona, A. Quattropani, and P. Schwendimann, Nonequilibrium dynamics of free quantum-well excitons in time-resolved photoluminescence, Phys. Rev. B **53**, 15834–15841 (1996).

[8] C. Piermarocchi, F. Tassone, V. Savona, A. Quattropani, and P. Schwendimann, Exciton formation rates in GaAs/Al$_x$Ga$_{1-x}$As quantum wells, Phys. Rev. B **55**, 1333–1336 (1997).

[9] J. Feldmann, G. Peter, E.O. Göbel, P. Dawson, K. Moore, C. Foxon, and R.J. Elliott, Linewidth dependence of radiative exciton lifetimes in quantum wells, Phys. Rev. Lett. **59**, 2337–2340 (1987).

[10] M. Gurioli, A. Vinattieri, M. Colocci, C. Deparis, J. Massies, G. Neu, A. Bosacchi, and S. Franchi, Temperature dependence of the radiative and nonradiative recombination time in GaAs/Al$_x$Ga$_{1-x}$As quantum-well structures, Phys. Rev. B **44**, 3115–3124 (1991).

[11] J. Martinez-Pastor, A. Vinattieri, L. Carraresi, M. Colocci, Ph. Roussignol, and G. Weimann, Temperature dependence of exciton lifetimes in GaAs/Al$_x$Ga$_{1-x}$As single quantum wells, Phys. Rev. B **47**, 10456–10460 (1993).

[12] R. Eccleston, B.F. Feuerbacher, J. Kuhl, W.W. Rühle, and K. Ploog, Density-dependent exciton radiative lifetimes in GaAs quantum wells, Phys. Rev. B **45**, 11403–11406 (1992).

[13] V. Srinivas, J. Hryniewicz, Y.J. Chen, and C.E.C. Wood, Intrinsic linewidths and radiative lifetimes of free excitons in GaAs quantum wells, Phys. Rev. B **46**, 10193–10196 (1992).

[14] B. Deveaud, F. Clérot, N. Roy, K. Satzke, B. Sermage, and D.S. Katzer, Enhanced radiative recombination of free excitons in GaAs quantum wells, Phys. Rev. Lett. **67**, 2355–2358 (1991).

[15] A. Vinattieri, J. Shah, T.C. Damen, D.S. Kim, L.N. Pfeiffer, M.Z. Maialle, and L.J. Sham, Exciton dynamics in GaAs quantum wells under resonant excitation, Phys. Rev. B **50**, 10868–10879 (1994).

[16] E. Hanamura, Rapid radiative decay and enhanced optical nonlinearity of excitons in a quantum well, Phys. Rev. B **38**, 1228–1234 (1988).

[17] L.C. Andreani, F. Tassone, and F. Bassani, Radiative lifetime of free excitons in quantum wells, Solid State Commun. **77**, 641–645 (1991).

[18] D.S. Citrin, Radiative lifetimes of excitons in quantum wells: Localization and phase-coherence effects, Phys. Rev. B **47**, 3832–3841 (1993).

[19] K. Muraki, Y. Takahashi, A. Fujiwara, S. Fukatsu, and Y. Shiraki, Enhancement of free-to-bound transitions due to resonant electron capture in

Be-doped AlGaAs/GaAs quantum wells, Solid State Electron. **37**, 1247–1250 (1994).

[20] G.A. Balchin, L.M. Smith, A. Petrou, and B.D. McCombe, Time-resolved polarized photoluminescence spectroscopy of confined donors in GaAs/Al$_x$Ga$_{1-x}$As quantum wells, Superlattices Microstruct. **18**, 291–296 (1995).

[21] J. Kundrotas, A. Čerškus, G. Valušis, E.H. Linfield, E. Johannessen, and A. Johannessen, Dynamics of free carriers – neutral impurity related optical transitions in Be and Si δ-doped GaAs/AlAs multiple quantum wells: Fractional-dimensional space approach, Lith. J. Phys. **54**, 233–243 (2014).

[22] J.P. Bergman, P.O. Holtz, B. Monemar, M. Sundaram, J.L. Merz, and A.C. Gossard, Decay measurements of free- and bound-exciton recombination in doped GaAs/Al$_x$Ga$_{1-x}$As quantum wells, Phys. Rev. B **43**, 4765–4770 (1991).

[23] C.I. Harris, B. Monemar, H. Kalt, P.O. Holtz, M. Sundaram, J.L. Merz, and A.C. Gossard, Exciton dynamics in GaAs/Al$_x$Ga$_{1-x}$As doped quantum wells, Phys. Rev. B **50**, 18367–18374 (1994).

[24] T. Matsusue and H. Sakaki, Radiative recombination coefficient of free carriers in GaAs-AlGaAs quantum wells and its dependence on temperature, Appl. Phys. Lett. **50**, 1429–1431 (1987).

[25] P.J. Bishop, M.E. Daniels, B.K. Ridley, and K. Woodbridge, Radiative recombination in GaAs/Al$_x$Ga$_{1-x}$As quantum wells, Phys. Rev. B **45**, 6686–6691 (1992).

[26] J.W. Orton, P. Dawson, D.E. Lacklison, T.S. Cheng, and C.T. Foxon, Recombination lifetime measurements in AlGaAs/GaAs quantum well structures, Semicond. Sci. Technol. **9**, 1616–1622 (1994).

[27] N.F. Mott, *Metal-Insulator Transitions*, 2nd ed. (Taylor & Francis, London, 1990).

[28] J. Kundrotas, A. Čerškus, G. Valušis, M. Lachab, S.P. Khanna, P. Harrison, and E.H. Linfield, Radiative recombination spectra of *p*-type δ-doped GaAs/AlAs multiple quantum wells near the Mott transition, J. Appl. Phys. **103**, 123108 (2008).

[29] J. Kundrotas, A. Čerškus, G. Valušis, L.H. Li, E.H. Linfield, A. Johannessen, and E. Johannessen, Light emission lifetimes in *p*-type δ-doped GaAs/AlAs multiple quantum wells near the Mott transition, J. Appl. Phys. **112**, 043105 (2012).

[30] A. Čerškus, J. Kundrotas, G. Valušis, P. Harrison, S. Khanna, and E. Linfield, Formation of low energy tails in silicon δ-doped GaAs/AlAs multiple quantum wells, Proc. SPIE **6596**, 659613 (2007).

[31] J. Kundrotas, A. Čerškus, S. Ašmontas, G. Valušis, B. Sherliker, M.P. Halsall, M.J. Steer, E. Johannessen, and P. Harrison, Excitonic and impurity-related optical transitions in Be δ-doped GaAs/AlAs multiple quantum wells: Fractional-dimensional space approach, Phys. Rev. B **72**, 235322 (2005).

[32] J. Kundrotas, A. Čerškus, G. Valušis, A. Johannessen, E. Johannessen, P. Harrison, and E.H. Linfield, Impurity-related photoluminescence line shape asymmetry in GaAs/AlAs multiple quantum wells: Fractional-dimensional space approach, J. Appl. Phys. **107**, 093109 (2010).

[33] H.W. Yoon, D.R. Wake, and J.P. Wolfe, Effect of exciton-carrier thermodynamics on the GaAs quantum well photoluminescence, Phys. Rev. B **54**, 2763–2774 (1996).

EKSITONINĖS SPINDULIUOTĖS GESIMO TRUKMIŲ MATAVIMAI VIDUTINIŠKAI δ-LEGIRUOTUOSE GaAs/AlAs KARTOTINIUOSE KVANTINIUOSE ŠULINIUOSE

J. Kundrotas [a], A. Čerškus [a], G. Valušis [a], E.H. Linfield [b], E. Johannessen [c], A. Johannessen [c]

[a] *Fizinių ir technologijos mokslų centro Puslaidininkių fizikos institutas, Vilnius, Lietuva*
[b] *Lidso universitetas, Lidsas, Jungtinė Karalystė*
[c] *Buskerudo ir Vestfoldo universitetinis koledžas, Borre, Norvegija*

Santrauka

Šiame darbe tirtos kartotinės kvantinės duobės buvo užaugintos molekulinių pluoštelių epitaksijos būdu ant didžiavaržių GaAs padėklų. Kvantinės GaAs 20 nm pločio duobės buvo atskirtos 5 nm pločio AlAs barjerais. Į kiekvienos kvantinės duobės vidurį buvo įterptas silicio (Si) donorinių arba berilio (Be) akceptorinių priemaišų δ sluoksnis.

Rekombinaciniai vyksmai buvo tirti plačiame temperatūrų intervale keičiant kvantinių duobių gardelės temperatūrą nuo 3,6 iki 300 K. Fotoliuminescencijos žadinimui naudojome diodu kaupinamą Nd:LSB kietojo kūno pikosekundinį lazerį. Dinaminiai fotoliuminescencijos vyksmai buvo tiriami naudojant koreliuotų pavienių fotonų skaičiavimo metodiką (TCSPC). Pagrindinis dėmesys skirtas laisvųjų eksitonų spinduliuotės gesimo trukmių tyrimui. Nustatyta, kad gesimo laikas sutrumpėja legiruotuose GaAs/AlAs kartotiniuose kvantiniuose šuliniuose. Jis priklauso nuo priemaišų tankio ir jų tipo: *n* ar *p*. Stipresnis gesimas stebimas *n* tipo bandiniuose esant mažesniems priemaišų tankiams. Prieita prie išvados, kad yra svarbūs kolektyviniai priemaišų reiškiniai, susiję su priemaišų banginių funkcijų persiklojimu ir Moto dielektrikas–metalas virsmu. *n* tipo priemaišoms būdinga mažesnė jonizacijos energija bei didesnis Boro radiusas lyginant su *p* tipo priemaišomis. Kolektyviniai reiškiniai pasireiškia *n* tipo kvantiniuose šuliniuose esant mažesniems tankiams.